

Arrival Time Distributions of Spin-1/2 Particles

Siddhant Das* and Detlef Dürr†

Mathematisches Institut, Ludwig-Maximilians-Universität München,
Theresienstr. 39, D-80333 München, Germany

(Dated: February 21, 2018)

The arrival time statistics of spin-1/2 particles governed by Pauli's equation, and defined by their Bohmian trajectories, show unexpected and very well articulated features. Comparison with other proposed statistics of arrival times that arise from either the usual quantum flux or from semiclassical considerations suggest testing these notable deviations in an *experimentum crucis* of the validity of the Bohmian predictions for spin-1/2 particles. The suggested experiment, including the preparation of the wave functions, could be done with present-day experimental technology.

In non-relativistic quantum mechanics, the probability of finding a particle in a small spatial volume d^3r around position \mathbf{r} at a fixed time t is given by Born's rule $|\psi(\mathbf{r}, t)|^2 d^3r$, where $\psi(\mathbf{r}, t)$ is the wave function of the particle. This formula is experimentally well established. However, a formula for the probability of finding the particle at a fixed point \mathbf{r} between times t and $t + dt$ is the matter of an ongoing debate [1–4]. Although it has often been observed that there is no time observable in quantum mechanics [5], it is commonly accepted by now that measurements of time are clearly possible. Let us consider a typical time of arrival experiment, in which a particle is initially trapped in a region $\Sigma \subset \mathbb{R}^3$, e.g., the interior of a potential well. The trap is released at, say, $t = 0$ allowing the particle to propagate freely in space. If the trapping potential is deep enough, the wave function of the particle at this instant, $\Psi_0(\mathbf{r}) \equiv \Psi(\mathbf{r}, t = 0)$, practically vanishes outside the region Σ . Particle detectors placed on the boundary $\partial\Sigma$ measure the time of (first) arrival of the particle, denoted by τ . If the experiment is repeated many times, the recorded arrival times are random, even if the initial wave function of the particle (Ψ_0) is kept unchanged in each experiment. What is the probability distribution of arrival times $\Pi^{\Psi_0}(\tau)$ as a functional depending on Ψ_0 and on $\partial\Sigma$?

There are various problems with finding a general formula for $\Pi^{\Psi_0}(\tau)$, i.e., a tractable formula applicable to all wave functions. From an operational perspective the statistics of detector clicks in an arrival time experiment must be given by a positive operator valued measure (POVM) on the particle's Hilbert space, but what it is and whether it is the same for all measurement devices is unclear (see [6, 7] for a discussion). One problem is that detection events are always based on interactions of the apparatus with the detected particle that may change the particle's wave function by backscattering, leading in extreme cases to the quantum Zeno effect. On the other hand, the theoretical prediction for the first arrival time distribution $\Pi^{\Psi_0}(\tau)$, also referred to as the *ideal* or *intrinsic* distribution, should *a priori* be independent of the measurement apparatus. It is this distribution which should, for some well suited wave functions at least, be testable in experiments. Another problem arises from the

fact that the notion of arrival time is most naturally connected with that of particle trajectories, an idea which is hard to concretize in the orthodox interpretation of quantum mechanics.¹ It is hence difficult to derive a unique formula for $\Pi^{\Psi_0}(\tau)$ from first principles, see [1, 2, 7, 9] for various attempts. Moreover, recent attoclock experiments (measuring the tunnel delay time of ionized electrons) have shown some of the theoretical contenders to be empirically inadequate [10, 11].

Bohmian mechanics is a quantum theory where particles move on well defined trajectories and which is proven to be empirically equivalent to standard quantum mechanics, wherever the latter is *unambiguous* [12, 13]. The issue of arrival times may thus become an *experimentum crucis*. We suggest here such an experiment. We find that the Bohmian arrival times of a spin-1/2 particle in certain experimentally accessible setups show drastic and unexpected changes when control parameters are changed.

Our suggested experimental setup is this: A spin-1/2 particle of mass m is constrained to move within a semi-infinite cylindrical waveguide. Initially, it is trapped between the end face of the waveguide and an impenetrable potential barrier placed at a distance d . At the start of the experiment, the particle is prepared in a ground state Ψ_0 of this cylindrical box, then the barrier at d is suddenly switched off, allowing the particle to propagate freely within the waveguide. The arrival surface $\partial\Sigma$ is the *plane* situated at distance $L (> d)$ from the end face of the waveguide. We then compute *numerically* from the Bohmian equations of motion how long it takes for the particle to arrive at $\partial\Sigma$, and determine the empirical distribution $\Pi_{\text{Bohm}}^{\Psi_0}(\tau)$ from *typical* trajectories² for different initial ground state wave functions. We find that

- (i) If the initial wave function of the particle has only one non-zero component – a “spin-up” or “spin-

¹ See however Kocsis et al. [8] for a *weak* measurement of trajectories, which can indeed be seen as Bohmian trajectories.

² trajectories whose initial points are randomly drawn from the Born $|\Psi_0|^2$ distribution.

down” wave function³– the arrival time distribution $\Pi_{\text{Bohm}}^{\Psi_0}(\tau)$ coincides with the quantum flux expression

$$\int_{\partial\Sigma} \mathbf{J}_{\text{Pauli}}(\mathbf{r}, \tau) \cdot d\mathbf{s} =: \Pi_{\text{qf}}(\tau), \quad (1)$$

where $\mathbf{J}_{\text{Pauli}}(\mathbf{r}, \tau)$ is the quantum flux (or probability current density) of the Pauli wave equation (cf Eq. (3)). This distribution has a heavy tail $\sim \tau^{-4}$ as $\tau \rightarrow \infty$. Note well that by the very meaning of the quantum flux, (1) is a natural guess for the arrival time distribution from the point of view of standard quantum mechanics [3] as well. But note also that (1) makes sense *only* if the left-hand side is positive, which need not be the case. However, in our case it is non-negative for the aforementioned wave functions.

- (ii) For other initial wave functions these distributions are different from (1) and fall off faster than $\sim \tau^{-4}$. For any initial ground state wave function, the arrival time distribution displays an infinite sequence of *self-similar* lobes below $\tau = \frac{m d L}{2\pi\hbar}$ (see Fig. 1 below), which diminish in size as $\tau \rightarrow 0$. These lobes mirror typical wave function evolution when suddenly released to spread freely into the volume of the waveguide (see also [14]).
- (iii) If the initial wave function is an *equal superposition* of the spin-up and spin-down wave functions, the arrival time distribution pinches off at a maximum arrival time τ_{max} , i.e., *no* particle arrivals occur for $\tau > \tau_{\text{max}}$. Opposed to (ii), the behaviour of trajectories lead in this case to an even more striking manifestation of the lobes: characteristic “no-arrival *windows*” appear between the smaller lobes, inside which the arrival time distribution is *zero*.
- (iv) All distributions deviate significantly from the alleged semiclassical formula.

We briefly summarize the Bohmian mechanics of spin-1/2 particles. For such a particle the wave function $\Psi(\mathbf{r}, t)$ is a two-component complex-valued spinor solution of the Pauli equation

$$i\hbar \frac{\partial}{\partial t} \Psi(\mathbf{r}, t) = -\frac{\hbar^2}{2m} (\boldsymbol{\sigma} \cdot \nabla)^2 \Psi(\mathbf{r}, t) + V(\mathbf{r}, t) \Psi(\mathbf{r}, t), \quad (2)$$

with some initial condition $\Psi_0(\mathbf{r})$. Here, $V(\mathbf{r}, t)$ is an external potential, and $\boldsymbol{\sigma} = \sigma_x \hat{\mathbf{x}} + \sigma_y \hat{\mathbf{y}} + \sigma_z \hat{\mathbf{z}}$ is a 3-vector of Pauli spin matrices. The quantum continuity

equation for the Pauli equation reads [15, 16]

$$\begin{aligned} \frac{\partial |\Psi|^2}{\partial t} &= \frac{\hbar}{m} \nabla \cdot \left(\text{Im}[\Psi^\dagger \nabla \Psi] + \frac{1}{2} \nabla \times (\Psi^\dagger \boldsymbol{\sigma} \Psi) \right) \\ &= \nabla \cdot \mathbf{J}_{\text{Pauli}} =: \nabla \cdot (\mathbf{v}_{\text{Bohm}}^\Psi |\Psi|^2), \end{aligned} \quad (3)$$

where Ψ^\dagger is the adjoint of Ψ , and $|\Psi|^2 = \Psi^\dagger \Psi$. The right-most equality of (3) defines the Bohmian velocity field⁴ $\mathbf{v}_{\text{Bohm}}^\Psi = \mathbf{J}_{\text{Pauli}}/|\Psi|^2$. The Bohmian trajectories are integral curves of the velocity field $\mathbf{v}_{\text{Bohm}}^\Psi$, hence the Bohmian *guidance law* reads

$$\begin{aligned} \frac{d}{dt} \mathbf{R}(t) &= \mathbf{v}_{\text{Bohm}}^\Psi(\mathbf{R}(t), t) = \frac{\hbar}{m} \text{Im} \left[\frac{\Psi^\dagger \nabla \Psi}{\Psi^\dagger \Psi} \right] (\mathbf{R}(t), t) \\ &\quad + \frac{\hbar}{2m} \left[\frac{\nabla \times (\Psi^\dagger \boldsymbol{\sigma} \Psi)}{\Psi^\dagger \Psi} \right] (\mathbf{R}(t), t). \end{aligned} \quad (4)$$

Here, $\mathbf{R}(t)$ is the position of the particle at time t . The first term on the right-hand side of (4) is known as the *convective-velocity*, while the second term is called the *spin-velocity* or the *Gordon-velocity*. In Bohm’s theory, the spin-1/2 particle has no degrees of freedom other than those specifying its position in space, so spin is not an *extra* degree of freedom. Thus, all quantum mechanical phenomena attributed to spin (such as the deflection of particles in the Stern-Gerlach experiment) arise solely from the non-linear equation of motion [19, 20]. The guidance law (4) is time reversal invariant and its right-hand side transforms as a velocity under Galilean transformations (see [12, 17] for further discussion). We integrate Eq. (4) for a statistical ensemble of $|\Psi_0|^2$ -distributed initial particle positions $\mathbf{R}(0)$.⁵ The random first arrival time τ is then simply the time at which the random Bohmian trajectory $\mathbf{R}(t, \mathbf{R}(0))$ strikes the surface $\partial\Sigma$.

We turn now to the details of our computations and results. Let the cylindrical waveguide be mounted on the xy -plane of a right-handed orthogonal coordinate system, the axis of the cylinder defining the z -axis. Employing cylindrical coordinates $\mathbf{r} \equiv (r, \phi, z)$, we model the potential field of the waveguide as $V(\mathbf{r}, t) = V_\perp(r) + V_\parallel(z, t)$, where $V_\perp(r) = \frac{1}{2} m \omega^2 r^2$ is a transverse confining potential and $V_\parallel(z, t) = v(z) + \theta(-t)v(d-z)$ is a time dependent axial potential, comprised of an impenetrable

³ Here, “spin up” is w.r.t. to the waveguide axis.

⁴ The alert reader will immediately recognize that the divergence of the $\boldsymbol{\sigma}$ -summand on the right-hand side of (3) is zero, hence one may argue that neither the flux nor the Bohmian velocity are uniquely defined. However, observing that the Pauli equation and its flux $\mathbf{J}_{\text{Pauli}}$ emerge as nonrelativistic limits of the Dirac equation and the Dirac flux, respectively, which are unique [17, 18], one is led directly to the current and Bohmian velocity given here.

⁵ It has actually been proven that the initial position of a Bohmian particle is distributed according to Born’s statistical rule [21].

hard wall at $z = 0$, viz.,

$$v(z) = \begin{cases} \infty & z \leq 0 \\ 0 & z > 0 \end{cases}, \quad (5)$$

and another impenetrable potential barrier $v(d - z)$ that is switched off at $t = 0$. The wall at $z = 0$ denotes the end face of the waveguide and $\theta(x)$ is Heaviside's step function.

Fortunately, near perfect harmonic confinements can be realized in conventional (ultrahigh vacuum) Penning traps, which can trap single electrons [22, 23] and protons [24] over a wide range of trapping frequencies. For electrons, typical waveguide parameters read: $L \approx 6 - 10$ mm, $\omega \approx 70 - 880$ GHz [22, 25].

For simplicity, we assume that the particle is prepared in a ground state of the cylindrical box at $t = 0$, which can be written as $\Psi_0(\mathbf{r}) = \psi_0(\mathbf{r})\chi$, where (setting $\hbar = m = d = 1$),

$$\psi_0(\mathbf{r}) = \sqrt{\frac{2\omega}{\pi}} \theta(z)\theta(1 - z) \sin(\pi z) \exp\left(-\frac{\omega}{2}z^2\right) \quad (6)$$

is the spatial part of the wave function, and

$$\chi = \begin{pmatrix} \cos(\alpha/2) \\ \sin(\alpha/2) e^{i\beta} \end{pmatrix}, \quad 0 \leq \alpha \leq \pi, \quad 0 \leq \beta < 2\pi, \quad (7)$$

is a normalized Bloch spinor ($\chi^\dagger\chi = 1$). Fixing α and β , we obtain different ground state wave functions. For instance, $\alpha = 0$ (π) gives the spin-up (spin-down) ground state wave function, usually denoted by Ψ_\uparrow (Ψ_\downarrow), while $\alpha = \frac{\pi}{2}$ and $\beta = 0$ yields the so-called up-down ground state wave function $\Psi_\updownarrow = \frac{1}{\sqrt{2}}(\Psi_\uparrow + \Psi_\downarrow)$. We refer to α and β as *spin orientation angles*, because they specify the orientation of the ‘‘spin vector’’

$$\mathbf{s} := \frac{1}{2} \begin{pmatrix} \Psi^\dagger \boldsymbol{\sigma} \Psi \\ \Psi^\dagger \Psi \end{pmatrix} = (\sin \alpha \cos \beta \hat{\mathbf{x}} + \sin \alpha \sin \beta \hat{\mathbf{y}} + \cos \alpha \hat{\mathbf{z}})$$

associated with the initial wave function Ψ_0 .

$$\mathcal{D}(x, t) := \frac{e^{-i\frac{\pi}{2}t}}{8i} \left\{ e^{i\pi x} \operatorname{erfc} \left[\frac{i^{3/2}}{\sqrt{2}} \left(\frac{x}{\sqrt{t}} - \pi\sqrt{t} \right) \right] - e^{-i\pi x} \operatorname{erfc} \left[\frac{i^{3/2}}{\sqrt{2}} \left(\frac{x}{\sqrt{t}} + \pi\sqrt{t} \right) \right] \right\}, \quad (12)$$

where $\operatorname{erfc}(x)$ is the complementary error function. A detailed derivation of this result will be given elsewhere.

Substituting our solution for the time dependent wave function in the guidance law (4), we obtain coupled non-

The instant the barrier is switched off, the wave function spreads dispersively, filling the volume of the waveguide. The particle moves according to (4) on the Bohmian trajectory $\mathbf{R}(t) = R(t) [\cos \Phi(t) \hat{\mathbf{x}} + \sin \Phi(t) \hat{\mathbf{y}}] + Z(t) \hat{\mathbf{z}}$. In this choice of coordinates the first arrival time of a trajectory starting at $\mathbf{R}(0)$ and arriving at $z = L$ is

$$\tau(\mathbf{R}(0)) = \inf \{t \mid Z(t, \mathbf{R}(0)) = L, \mathbf{R}(0) \in \operatorname{supp}(\Psi_0)\}, \quad (8)$$

where $Z(t, \mathbf{R}(0)) \equiv Z(t)$ is the z -coordinate of the particle at time t , and $\operatorname{supp}(\Psi_0)$ denotes the support of the initial wave function (the interior of the cylindrical box).

Since the initial position $\mathbf{R}(0)$ is $|\Psi_0|^2$ -distributed, the distribution of $\tau(\mathbf{R}(0))$ is given as usual by

$$\Pi_{\text{Bohm}}^{\Psi_0}(\tau) = \int_{\operatorname{supp}(\Psi_0)} d^3\mathbf{R}(0) \delta(\tau(\mathbf{R}(0)) - \tau) |\Psi_0|^2(\mathbf{R}(0)). \quad (9)$$

In general, we do not have a nice closed expression for (8), hence the integral in (9) cannot be evaluated analytically. However, if the Bohmian trajectories cross $\partial\Sigma$ at *most* once, or in other words if the quantum flux $\mathbf{J}_{\text{Pauli}}$ is outward directed at *every point* of $\partial\Sigma$, at *all times* (the *current positivity* condition), then $\Pi_{\text{Bohm}}^{\Psi_0}(\tau)$ reduces to $\Pi_{\text{qf}}(\tau)$ [3, 4]. Also, in this case the left-hand side of (1) ≥ 0 . Generally, this condition is not met, and one can typically at best approximate $\Pi_{\text{Bohm}}^{\Psi_0}(\tau)$ from a large number of Bohmian trajectories, which must be *computed numerically*.

In this regard, observe that the Pauli equation (2) with initial condition Ψ_0 can be solved in closed form, facilitating very fast numerical computation of Bohmian trajectories. The time dependent wave function takes the form $\Psi(\mathbf{r}, t) = \psi(\mathbf{r}, t)\chi$, where the spin part (cf Eq. (7)) remains unchanged, while the spatial part

$$\psi(\mathbf{r}, t) = \sqrt{\frac{2\omega}{\pi}} \exp\left(-\frac{\omega}{2}z^2 - i\omega t\right) W(z, t), \quad (10)$$

where

$$W(z, t) = \theta(z) [\mathcal{D}(z - 1, t) + \mathcal{D}(1 - z, t) - \mathcal{D}(1 + z, t) - \mathcal{D}(-1 - z, t)], \quad (11)$$

which we call the ‘time evolution integral’. In (11):

linear equations of motion for the spin-1/2 particle:

$$\dot{R}(t) = \sin \alpha \sin(\Phi(t) - \beta) \operatorname{Re} \left[\frac{W'}{W} \right] (Z(t), t), \quad (13a)$$

$$\dot{\Phi}(t) = \frac{\sin \alpha}{R(t)} \cos(\Phi(t) - \beta) \operatorname{Re} \left[\frac{W'}{W} \right] (Z(t), t) + \omega \cos \alpha, \quad (13b)$$

$$\dot{Z}(t) = \operatorname{Im} \left[\frac{W'}{W} \right] (Z(t), t) + \omega \sin \alpha \sin(\Phi(t) - \beta) R(t), \quad (13c)$$

where $W' = \partial W / \partial z$.

In order to determine $\Pi_{\text{Bohm}}^{\Psi_0}(\tau)$ (henceforth denoted by $\Pi_{\text{Bohm}}^{\alpha|\beta}(\tau)$ for brevity) we sample N initial positions from the $|\Psi_0|^2$ distribution, solve Eq. (13) numerically for each point in this ensemble, continuing until the trajectory hits $z = L$, then record the arrival time. For N large, the histogram of arrival times approximates $\Pi_{\text{Bohm}}^{\alpha|\beta}(\tau)$.

Before presenting particular numerical results, we quote two remarkable properties of $\Pi_{\text{Bohm}}^{\alpha|\beta}(\tau)$, viz.,

$$\Pi_{\text{Bohm}}^{\alpha|\beta}(\tau) = \Pi_{\text{Bohm}}^{\alpha|0}(\tau), \quad (14a)$$

$$\Pi_{\text{Bohm}}^{\alpha|\beta}(\tau) = \Pi_{\text{Bohm}}^{\pi-\alpha|\beta}(\tau). \quad (14b)$$

These are enough to show that there is no loss in generality in setting $\beta = 0$ in all that follows.⁶

For the spin-up and spin-down wave functions, Eq. (13c) reduces to $\dot{Z} = \operatorname{Im}[W'/W](Z(t), t)$, therefore when the particle crosses $\partial\Sigma$, $\dot{Z} = \operatorname{Im}[W'/W](L, t) > 0$.⁷ This implies that the spin-up and spin-down trajectories cross $\partial\Sigma$ at most once, and as a result the arrival time distribution in these cases equals $\Pi_{\text{qf}}(\tau)$. It can also be computed explicitly (cf Eq. (1)), viz.,

$$\Pi_{\text{qf}}(\tau) = 2 \operatorname{Im}[W^*(L, \tau)W'(L, \tau)]. \quad (15)$$

As indicated earlier, (15) is non-negative for all values of τ , and features prominently a large main lobe for $\tau > \frac{L}{2\pi}$. The main lobe falls off as

$$\left(\frac{L}{\pi}\right)^3 \frac{4}{\tau^4}, \quad \text{as } \tau \rightarrow \infty. \quad (16)$$

An infinite train of smaller lobes permeates the interval $0 < \tau < \frac{L}{2\pi}$, which are well approximated by the formula

$$\frac{4\pi}{L} \operatorname{sinc}^2\left(\frac{L}{\tau}\right), \quad \text{whenever } \tau \ll L. \quad (17)$$

$\Pi_{\text{qf}}(\tau)$ is graphed in Fig. 1 for $L = 100$. In this figure the numerically obtained spin-up arrival time histogram is depicted alongside, which clearly agrees with (15). Note that $\Pi_{\text{qf}}(\tau)$ is a function *only* of the arrival distance L . In particular, it is independent of the trapping frequency ω , which is rather surprising. We also find that the spin-up (down) arrival time statistics are independent of the

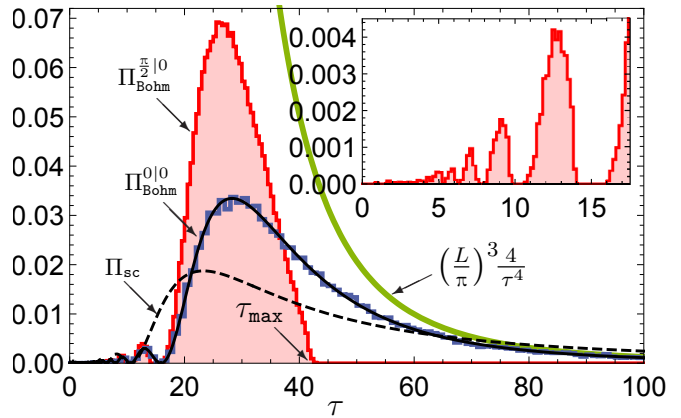


FIG. 1. Arrival time histograms for spin-up ($\alpha = 0$) and up-down ($\alpha = \frac{\pi}{2}$) wave functions, with $\beta = 0$, $L = 100$ and $\omega = 10^3$ graphed along with the semiclassical arrival time distribution $\Pi_{\text{sc}}(\tau)$ (dashed line). Inset: Magnified view of the self-similar smaller lobes of the up-down histogram, separated by distinct no-arrival windows. The arrival time histogram for the spin-up wave function agrees with the quantum flux $\Pi_{\text{qf}}(\tau)$ (solid line). For the up-down case, no arrivals are recorded for $\tau > 42.8943$ ($= \tau_{\text{max}}$). Each histogram in this figure has been generated with 10^5 Bohmian trajectories. The time scale on the horizontal axis is $\approx 21.6 \mu\text{s}$, assuming $d = 50 \mu\text{m}$.⁸

exact shape of the transverse confining potential $V_{\perp}(z)$ of the waveguide as well.

We turn now to the results for other ground state wave functions. In light of Eq. (14b), we need only consider wave functions with $0 < \alpha \leq \frac{\pi}{2}$. First, note that the integrated flux (1) corresponding to these wave functions *also* equals (15), yet the respective arrival time distributions do *not* agree with the same. This is because the Bohmian trajectories in these cases cross $\partial\Sigma$ more than once, hence the aforementioned current positivity condition is not met.

As α approaches $\frac{\pi}{2}$, deviations from $\Pi_{\text{qf}}(\tau)$ become visible. In particular, the tail of $\Pi_{\text{Bohm}}^{\alpha|0}(\tau)$ thins gradually, pinching off completely at a characteristic maximum arrival time τ_{max} for $\alpha = \frac{\pi}{2}$ (see Fig. 1), i.e. *no* particle arrivals occur with $\tau > \tau_{\text{max}}$. This behavior results in a sharp drop in the mean arrival time $\langle \tau \rangle$ in the vicinity of $\alpha = \frac{\pi}{2}$, as shown in Fig. 2.

Unlike the spin-up (down) case, the up-down arrival time statistics are influenced by the trapping frequency ω . Keeping L fixed, we find that the maximum arrival time τ_{max} , mean arrival time $\langle \tau \rangle$, and the standard deviation σ corresponding to $\Pi_{\text{Bohm}}^{\frac{\pi}{2}|0}(\tau)$ decrease with increasing ω , each approaching a constant for large values of ω (see Fig. 3b). Conversely, when these quantities are graphed as functions of L with ω fixed (Fig. 3a), we see a clear linear growth in each.

Remarkably, these effects persist even for large L , provided ω is also made suitably large (a welcome feature for

⁶ Details of the proof will be presented elsewhere.

⁷ This inequality can be verified numerically from formula (11).

Penning traps). Increasing L causes the arrival time distributions to shift to larger values of τ , thus the smaller lobes can be easily seen, especially in experiments incapable of resolving very small arrival times. Figure 1 shows the arrival time statistics for $L = 100$ (≈ 5 mm for a $d = 50 \mu\text{m}$ trap) and $\omega = 10^3$ (≈ 46.3 MHz). The characteristic maximum arrival time $\tau_{\text{max}} \approx 42.8943$ for $\alpha = \frac{\pi}{2}$ corresponds to ≈ 0.926 ms.⁸

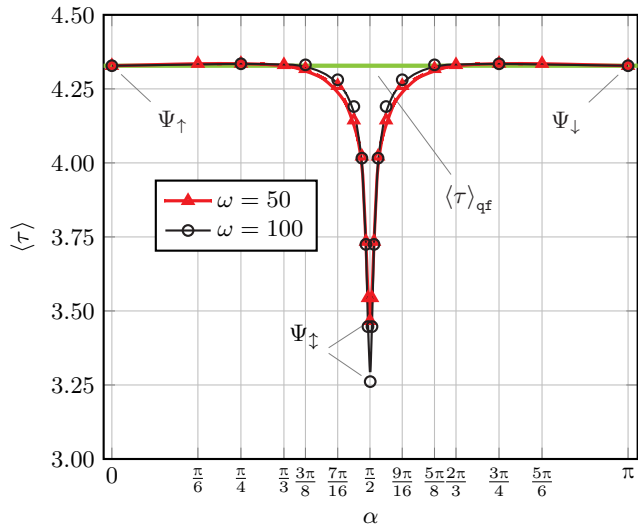


FIG. 2. Mean first arrival time $\langle \tau \rangle$ vs. spin orientation angle α for $L = 10$ and $\beta = 0$. The symmetry of the curves about $\alpha = \frac{\pi}{2}$ is a consequence of property (14b).

Since the smaller lobes become progressively thinner, resolving the n^{th} lobe (denoting the main lobe by $n = 1$) is limited by the least time count (δt) of the measuring apparatus. Roughly, $\delta t < \text{width of } n^{\text{th}} \text{ lobe}$ should suffice to resolve the first n lobes. This translates into

$$\delta t < \left(\frac{md}{\pi\hbar} \right) \frac{L}{n^2}. \quad (18)$$

For instance, taking $d = 50 \mu\text{m}$ and $L = 5$ mm (Fig. 1), a modest $\delta t \approx 10 \mu\text{s}$ will successfully resolve 8 lobes (main + 7 smaller lobes), while $\delta t \approx 0.1 \mu\text{s}$ will resolve as many as 83 lobes (main + 82 smaller lobes). However, we must also understand that only a few data points (about $\left(\frac{2}{\pi^2}\right) \frac{N}{n^4}$ in N experiments) contribute to the n^{th} lobe, especially when $n \gg 1$. This number, being independent of any tunable parameters like L , ω , etc., sets a fundamental limit on the experimenter's ability to resolve the distant lobes.

⁸ We have expressed L , ω and τ as multiples of d , $\frac{\hbar}{md^2}$ and $\frac{md^2}{\hbar}$, respectively. For a $d = 50 \mu\text{m}$ trap, known electron mass $m \approx 9.1094 \times 10^{-31} \text{ kg}$ and reduced Planck's constant $\hbar \approx 1.0546 \times 10^{-34} \text{ Js}$, the frequency and time units are $\approx 46.3 \text{ kHz}$ and $\approx 21.6 \mu\text{s}$, respectively.

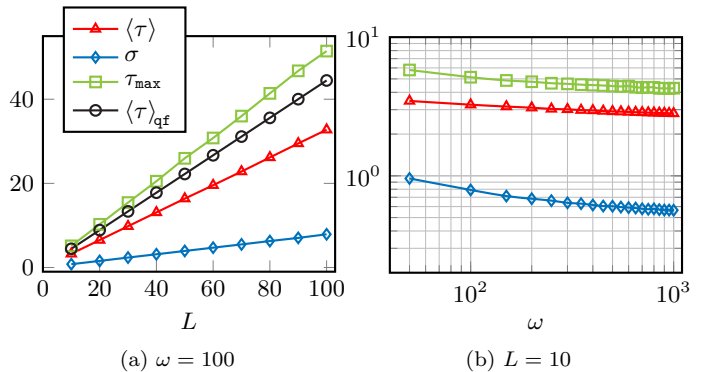


FIG. 3. (a) Graphs of mean arrival time $\langle \tau \rangle$, standard deviation σ and maximum arrival time τ_{max} for the up-down wave function vs. L , keeping ω fixed. The mean arrival time of $\Pi_{\text{qf}}(\tau)$ is also shown here. (b) Graphs of mean, standard deviation and maximum arrival time vs. ω , keeping L fixed.

Finally, we compare $\Pi_{\text{Bohm}}^{\alpha|\beta}(\tau)$ with the alleged semiclassical arrival time distribution

$$\Pi_{\text{sc}}(\tau) = \int_{\partial\Sigma} \frac{\mathbf{r} \cdot d\mathbf{s}}{\tau^4} \left| \tilde{\psi}_0 \left(\frac{\mathbf{r}}{\tau} \right) \right|^2, \quad (19)$$

routinely used in the interpretation of time-of-flight experiments. Here, $\tilde{\psi}_0$ denotes the Fourier transform of the initial wave function ψ_0 . Although (19) is based on the tacit assumption that the particle *moves classically* between preparation and measurement stages (see § 5.3.1 of [3]), it can also be motivated from the scattering formalism [4, pg 971], provided the detector surface ($\partial\Sigma$) is placed far away from the support of the initial wave function ψ_0 (far-field regime). In typical cold atom experiments these conditions are met, hence the semiclassical formula (19) is empirically adequate. Therefore, soliciting deviations from (19), theorists have recommended moving the “detectors closer to the region of coherent wave packet production, or closer to the interaction region” [2, 26, pg 419] (i.e. $L \approx d$). However, such a relocation may disturb the wave function of the particle in an undesirable way. For a meaningful comparison with our results, Eq. (19) (which is only applicable for free propagation) must be generalized to account for the presence of the waveguide. A careful calculation yields the formula

$$\Pi_{\text{sc}}(\tau) = \frac{8\pi L}{\tau^2} \frac{\cos^2(L/2\tau)}{((L/\tau)^2 - \pi^2)^2}, \quad (20)$$

which falls off as $\left(\frac{8}{\pi^3}\right) \frac{L}{\tau^2}$ (compare this with Eq. (16)). In Fig. 1, we see that the semiclassical formula (20) for $L = 100$ remains *distinctly different* from the Bohmian arrival time distributions, notwithstanding the largeness of L . Our predictions can thus be checked even in the far-field regime.

Bohmian mechanics has been fruitfully applied in various physical disciplines, for example, with reference to

technical advances [27–30], and to a better understanding of quantum phenomena even in quantum gravity [31]. We have proposed a simple experiment, the results of which orthodox quantum mechanics provides no unique way of predicting. A rather remarkable opportunity that could soon be tested thus presents itself. Our results demonstrate that the distribution of first arrival times of a spin-1/2 particle bears clear signatures of Bohm’s guidance law. The deviations of $\Pi_{\text{Bohm}}^{\Psi_0}(\tau)$ from the quantum flux distribution (1), so strikingly in evidence, are particularly noteworthy.

The authors would like to thank J. M. Wilkes for critically reviewing the manuscript. He and Markus Nöth verified our analytical calculations meticulously, which led to the correction of a mistake in the early stages of the work. The assistance of Grzesio Gradziuk and Leopold Kellers with the numerical simulations was essential, and greatly appreciated. Thanks are also due to Serj Aristarkhov, Lukas Nickel, Ward Struyve, Nikolai Leopold, Roderich Tumulka and Nicola Vona for inspiration and enriching discussions on the subject of this letter.

* Siddhant.Das@physik.uni-muenchen.de

† duerr@mathematik.uni-muenchen.de

- [1] J. G. Muga, R. S. Mayato, and Í. L. Egusquiza, eds., *Time in Quantum Mechanics*, 2nd ed., Lect. Notes Phys. 734, Vol. 1 (Springer, Berlin Heidelberg, 2008).
- [2] J. G. Muga and C. R. Leavens, Phys. Rep. **338**, 353 (2000).
- [3] P. Blanchard and J. Fröhlich, eds., *The Message of Quantum Science: Attempts Towards a Synthesis*, Lect. Notes Phys. 899 (Springer, Berlin Heidelberg, 2015) Chap. 5.
- [4] M. Daumer, D. Dürr, S. Goldstein, and N. Zanghì, J. Stat. Phys. **88**, 967 (1997).
- [5] B. Mielnik and G. Torres-Vega, Concepts of Physics. **II**, 81 (2005).
- [6] N. Vona, G. Hinrichs, and D. Dürr, Phys. Rev. Lett. **111**, 220404 (2013).
- [7] R. Tumulka, ArXiv e-prints (2016), arXiv:1601.03715.
- [8] S. Kocsis *et al.*, Science **332**, 1170 (2011).
- [9] J. M. Yearsley, J. Phys. Conf. Ser **306**, 012056 (2011).
- [10] A. S. Landsman *et al.*, Optica **1**, 343 (2014).
- [11] T. Zimmermann *et al.*, Phys. Rev. Lett. **116**, 233603 (2016).
- [12] D. Bohm and B. J. Hiley, *The Undivided Universe: An Ontological Interpretation of Quantum Theory* (Routledge, London and New York, 1993).
- [13] D. Dürr, S. Goldstein, and N. Zanghì, J. Stat. Phys. **116**, 959 (2004).
- [14] M. Moshinsky, Phys. Rev. **88**, 625 (1952).
- [15] M. S. Shikakhwa, S. Turgut, and N. K. Pak, Am. J. Phys. **79**, 1177 (2011).
- [16] W. B. Hodge, S. V. Migirditch, and W. C. Kerr, Am. J. Phys. **82**, 681 (2014).
- [17] P. R. Holland, Phys. Rev. A **60**, 4326 (1999).
- [18] P. R. Holland and C. Philippidis, Phys. Rev. A **67**, 062105 (2003).
- [19] C. Dewdney, P. R. Holland, and C. Kyprianidis, Phys. Lett. A **119**, 259 (1986).
- [20] C. Dewdney, P. R. Holland, C. Kyprianidis, and J. P. Vigièr, Nature **336**, 536 (1988).
- [21] D. Dürr, S. Goldstein, and N. Zanghì, J. Stat. Phys. **67**, 843 (1992).
- [22] D. Wineland, P. Ekstrom, and H. Dehmelt, Phys. Rev. Lett. **31**, 1279 (1973).
- [23] T. Joseph and G. Gabrielse, Appl. Phys. Lett. **55**, 2144 (1989).
- [24] S. Ulmer *et al.*, Phys. Rev. Lett. **106**, 253001 (2011).
- [25] H. G. Dehmelt, Rev. Mod. Phys. **62**, 525 (1990).
- [26] V. Delgado, Phys. Rev. A **59**, 1010 (1999).
- [27] D. Marian, N. Zanghì, and X. Oriols, Phys. Rev. Lett. **116**, 110404 (2016).
- [28] R. E. Wyatt, *Quantum dynamics with Trajectories: Introduction to Quantum Hydrodynamics* (Springer, New York, 2005).
- [29] X. Oriols and J. Mompart, eds., *Applied Bohmian Mechanics: From Nanoscale Systems to Cosmology* (Pan Stanford Publishing Pvt. Ltd., Singapore, 2012).
- [30] A. S. Sanz and S. Miret-Artés, eds., *A Trajectory Description of Quantum Processes*, 2nd ed., Lect. Notes Phys. 831, Vol. 2 (Springer, Berlin Heidelberg, 2014).
- [31] W. Struyve, Sci. Rep. **7** (2017), 10.1038/s41598-017-06616-y.